International Journal of Solids and Structures 48 (2011) 3431–3443

Contents lists available at SciVerse ScienceDirect

International Journal of Solids and Structures

journal homepage: www.elsevier.com/locate/ijsolstr

Stress-based nonlocal damage model

Cédric Giry, Frédéric Dufour *, Jacky Mazars

3SR, Grenoble-INP/UJF/CNRS, Domaine Universitaire, BP 53, 38041 Grenoble Cedex 9, France

ARTICLE INFO

Article history:
Received 4 November 2010
Received in revised form 9 July 2011
Available online 6 September 2011

Keywords:
Damage
Nonlocality
Interactions
Stress state

ABSTRACT

Progressive microcracking in brittle or quasi-brittle materials, as described by damage models, presents a softening behavior that in turn requires the use of regularization methods in order to maintain objective results. Such regularization methods, which describe interactions between points, provide some general properties (including objectivity and the non-alteration of a uniform field) as well as drawbacks (damage initiation, free boundary).

A modification of the nonlocal integral regularization method that takes the stress state into account is proposed in this contribution. The orientation and intensity of nonlocal interactions are modified in accordance with the stress state. The fundamental framework of the original nonlocal method has been retained, making it possible to maintain the method's advantages. The modification is introduced through the weight function, which in this modified version depends not only on the distance between two points (as for the original model) but also on the stress state at the remote point.

The efficiency of this novel approach is illustrated using several examples. The proposed modification improves the numerical solution of problems observed in numerical simulations involving regularization techniques. Damage initiation and propagation in mode I as well as shear band formation are analyzed herein.

1. Introduction

In quasi-brittle materials, nonlocality originates in the interactions between microcracks (Bažant, 1991) and leads to stress magnification in some of the areas surrounding a microcrack, thus allowing for the creation or growth of new microcracks. Nonlocal damage models aim to describe the behavior of quasi-brittle materials in microcracked areas that have not yet degenerated into a large open crack. In addition to restoring objectivity in numerical modeling for strain softening behavior, these models offer physical reliability to the results by explicitly introducing the nonlocal nature of microcracking.

Gradient-enhanced media (Peerlings et al., 1996) or the nonlocal integral method (Pijaudier-Cabot and Bažant, 1987), used as localization limiters, avoids the ill-posedness of governing equations of equilibrium and thus avoids mesh dependency. Both of these methods introduce an internal length into the constitutive law that may be related to the characteristic size of the material (i.e. aggregate size). In addition to this added length however, the nonlocal approach also explicitly introduces the shape of the interaction domain through the weight function shape. Peerlings et al. (2001) demonstrated that these two methods are strictly equivalent when Green's function is used as the weight function in the integral approach. Even though the shape of the weight function only plays a minor role in a 1D setting, we will still focus on the second approach since it provides greater flexibility and facilitates the introduction of non-isotropic nonlocalities by directly expressing the interactions between points within the weight function.

Nonlocal regularization methods are intended to determine global behavior of the structure as well as macrocracking according to a diffuse approach using the damage field. However, several drawbacks arise when using the original nonlocal model, namely:

(a) Damage initiation in the crack tip problem.
Eringen et al. (1977) exposed the crack tip problem in nonlocal elasticity. They indicated that the point subjected to maximum stress is not located at the crack tip. Simone et al. (2004) demonstrated that this problem leads to erroneous damage initiation due to an inaccurate prediction of the maximum nonlocal equivalent strain in the presence of a predefined notch. Jirasek et al. (2004) concluded that different strategies could be adopted in order to model the notch either explicitly by geometry or by filling it with a completely damaged material. Moreover, they were able to better fit the size effect on fracture energy in the case of a notch modeled as a layer of completely damaged material.

* Corresponding author. Tel.: +33 4 56 52 86 41; fax: +33 4 76 82 70 43.
E-mail address: Frederic.Dufour@hmg.inpg.fr (F. Dufour).

0020-7683/$ - see front matter © 2011 Elsevier Ltd. All rights reserved.
doi:10.1016/j.ijsolstr.2011.08.012

Nonetheless, it can be physically expected to observe the damage initiation and evolution from the crack tip and not along the notch, as would have been obtained with a layer of completely damaged material.

(b) Description of kinematic fields in the fracture process zone (FPZ).
The chosen method fails to represent open macrocracks with localized strains across the crack. The poor resolution of local quantities stems from the fact that the nonlocality introduced into the calculation is established during the damage process and depends solely on the distance between neighboring points. At total failure, interactions across the cracked zone remain activated, thus leading to the so-called "damage diffusion" process.

(c) Description of interactions in the vicinity of boundaries.
The isotropic and constant description of nonlocalities leads to an inadequate treatment of interactions in the vicinity of free boundaries (Krayani et al., 2009; Pijaudier-Cabot and Dufour, 2010). Since an open macrocrack can be regarded as a newly formed free boundary, the original formulation is also inappropriate to model complete failure of the material.

The interactions are expected to change according to the loading undergone by the medium. In the presence of an FPZ, the development of numerous microcracks can be observed in front of a FPZ, whereas when looking back to front, no microcrack is expected to appear due to unloading. Similarly, near the boundary of a solid as loading conditions are being modified, nonlocality would be expected to differ when compared to the nonlocality throughout the bulk of the material. To take into account these evolutions, the nonlocal interactions between points need to be modified.

To overcome these drawbacks, we are proposing a new nonlocal method designed to satisfy the following criteria:

- convergence to localized kinematic fields upon failure;
- better description of the interactions in a medium with a stress gradient;
- absence of nonlocal interactions across a crack and, more generally, in the vicinity of free boundaries.

Over the last decade, several proposals have been forwarded to address one or more of the problems exposed above. As regards gradient-enhanced media, Voyiadjis and Abu Al-Rub (2005) proposed for ductile materials, based on experimental observations, the dependence of the internal length on several parameters, such as dislocation density and more particularly the plastic strain. Their proposal leads to a decrease in the length scale parameter with an increase in plastic strain. This approach allows for the internal length to evolve with the microstructure, yet the interactions remain isotropic and thus prevent improvement in the treatment of free boundaries or oriented macrocracks.

Geers et al. (1998) introduced the notion of gradient activity to describe the transient behavior of nonlocal interactions. Compared to the original gradient-enhanced media with a constant size c of the interaction domain, such gradient activity induces an evolution, driven by the local equivalent strain, from zero for an unloaded material to c for high strain levels. According to this approach, points lying outside the localization area, due to a decrease in their equivalent strain, tend to become more local as their gradient activity (i.e. interaction domain) decreases. As a consequence, they tend to be less influenced by points within the localization area. This approach allows for convergence to a crack for both displacement and nonlocal fields, with no damage diffusion at high loading levels, by reducing nonlocalities in the unloaded material. However, according to Simone (priv. comm. 2011), this improvement does not solve the issue of damage initiation and shear band evolution described in Simone et al. (2004).

For damage models relying on a nonlocal integral regularization technique, new proposals are forwarded for the evolution of interactions with damage (Pijaudier-Cabot and Dufour, 2010, addressed in Desmorat et al. (2010) and described in detail in Desmorat and Gatuingt (2007)). For the first 2 authors, the distance between points is replaced by a distance that integrates damage along the path, so as to reflect the distance over which an elastic wave propagates. As damage increases, this distance virtually increases as well, leading to a progressive degradation of interactions. On the simple case of a 1D bar under tension, this approach gives rise to some interesting results, with a gradual reduction in area with increasing damage, leading to a localized area with damage equal to 1 (which can be viewed as a macrocrack). Implementation of this approach however would seem to be numerically costly for the 2D and 3D calculations. For each step, performing an integration along all possible paths between two Gauss points of the damage field is actually required. According to the second approach, interactions depend on an internal wave propagation time instead of the distance between points. As the material evolves, this propagation time is modified, leading to a similar result of progressive degradation of interactions between points around a damaged area. A number of pending issues remain however with this approach regarding the choice of wave used and wave interactions with the boundaries. Furthermore, this approach remains computationally time-consuming.

Bažant et al. (2010) recently proposed a modification to the description of the nonlocal field in order to overcome boundary condition problems. These authors use a layer of local finite elements along a boundary, which can be perceived as the introduction of a zero internal length in the boundary layer. This approach considers an attenuation of the nonlocalities close to a boundary. Since the behavior remains isotropic however, the fracture process zone (FPZ) width close to boundaries is equal to the element size; moreover, mesh dependencies are introduced for crack initiation close to boundaries. Finally, the approach does not take into account the creation of new boundaries as macrocracks, which should modify the nonlocal interactions.

By considering developments on the interactions of microcracks at the origin of nonlocality, Bažant (1994) has proposed modifying the nonlocal method by adding a term to the original set-up that depends on the principal stress directions, as based on interactions between penny-shaped cracks. Depending on the stress directions, microcracks will be more or less activated and may magnify the surrounding stress state by means of interactions with neighboring microcracks. The redistributions are no longer isotropic, which tends to enhance the nonlocality description. Yet this approach also maintains a minimum interaction weight corresponding to the original nonlocal method, though this does not avoid residual interactions between points on both sides of a crack upon complete failure or the improper treatment of boundaries.

More recently, Krayani et al. (2009) proposed modifying the domain of interactions in the vicinity of boundaries. They focused on micromechanical considerations relative to interactions between circular voids using the analytical method developed by Kachanov (1987), according to which the stress redistribution due to interactions (nonlocal stress) should decrease in the vicinity of boundaries in the direction normal to these boundaries (Pijaudier-Cabot and Dufour, 2010). At its limit, the nonlocality is null in the normal direction of the boundary for a point located on the boundary.

This last proposal forms the basis of the work presented here in the specific case of a free boundary. This method seeks to properly describe nonlocal interactions in the vicinity of boundaries, leading to an improved description of FPZ initiation and thus a better assessment of size effects Krayani et al. (2009). These

modifications however only consider specimen geometry and do not allow for an evolution in interactions during the damage process. The nonlocal regularization domain is in fact modified solely in the vicinity of explicitly defined cracks. Newly damaged areas do not affect the regularization since new boundaries are not being created in the model.

In the present contribution, we suggest to enhance the nonlocal method proposed by Krayani et al. (2009) by providing a broader framework. To take into account the evolution of nonlocalities in the medium, we introduce a modification of interactions that depends on the principal stress directions, as proposed by Bažant (1994); furthermore, the intensity of interactions is proportional to the stress magnitude. An area under low stress will not influence its vicinity (e.g. normal to a free boundary or to a fully damaged zone).

The nonlocal damage model used in our study will be briefly recalled before introducing modifications of the regularization method. A test will then be performed on a notched plate under tension, in comparing the original and stress-based nonlocal methods as regards damage initiation and propagation.

Lastly, a shear band analysis of a specimen under compression will be performed so as to compare the efficiency of both methods in determining damage evolution.

2. Nonlocal damage model

2.1. Continuum damage theory

A scalar isotropic damage model for describing the non-linear behavior of concrete under monotonic loading has been used herein.

The general stress–strain relationship is:

$$\sigma_{ij} = (1 - D)C_{ijkl} : \varepsilon_{kl} \tag{1}$$

where σ_{ij} and ε_{kl} are the components of the Cauchy stress tensor and the strain tensor, respectively ($i, j, k, l \in [1,3]$) and C_{ijkl} are the components of the fourth-order elastic tensor. D is a scalar damage variable that quantifies material degradation; its value rises from 0 (for a virgin material) to 1 (completely degraded material).

The evolution in D is driven by an equivalent strain ε_{eq} that quantifies the local deformation state in the material. Among several definitions, this paper will consider the equivalent strain defined by de Vree et al. (1995) with the evolution law proposed by Peerlings et al. (1998)). The scalar damage variable D is a function of the internal variable Y; this parameter initially equals the damage threshold ε_{D_0} and is the largest recorded value of ε_{eq} during the damage process. This evolution is governed by the Kuhn–Tucker condition:

$$\varepsilon_{eq} - Y \leqslant 0, \quad \dot{Y} \geqslant 0, \quad \dot{Y}(\varepsilon_{eq} - Y) = 0 \tag{2}$$

The equivalent strain is based on the von Mises strain (de Vree et al., 1995):

$$\varepsilon_{eq} = \frac{k-1}{2k(1-2\nu)} I_1 + \frac{1}{2k}\sqrt{\frac{(k-1)^2}{(1-2\nu)^2} I_1^2 + \frac{12k}{(1+\nu)^2} J_2'} \tag{3}$$

with ν being the Poisson's ratio and I_1 and J_2' two invariants of the strain tensor $\boldsymbol{\varepsilon}$ defined as:

$$I_1 = tr(\boldsymbol{\varepsilon}) = \varepsilon_1 + \varepsilon_2 + \varepsilon_3 \tag{4}$$

$$J_2' = \frac{1}{6}(3tr(\boldsymbol{\varepsilon} \cdot \boldsymbol{\varepsilon}) - tr^2(\boldsymbol{\varepsilon})) \tag{5}$$

Parameter k corresponds to the ratio of compressive strength to tensile strength.

The damage evolution law introduced is the one proposed by Peerlings et al. (1998):

$$D = 1 - \frac{\varepsilon_{D_0}}{Y}(1 - \alpha + \alpha \exp(-\beta(Y - \varepsilon_{D_0}))) \tag{6}$$

with α and β parameters governing the shape of this evolution law. An exponential damage evolution law has been chosen in order to reach high damage levels at very low stress levels, thus avoiding use of an erosion technique or other methods necessary to execute a calculation in the case of damage evolution with D equal to 1 at a finite strain.

This constitutive relation exhibits strain softening and, as a consequence, requires a regularization technique (see for a complete review Bažant and Jirasek (2002)).

2.2. Original integral nonlocal approach

In the nonlocal damage model, the equivalent strain given in Eq. (3) is replaced by an average equivalent strain $\bar{\varepsilon}_{eq}$ over a volume Ω in the equation governing the extension of damage as defined by Pijaudier-Cabot and Bažant (1987):

$$\bar{\varepsilon}_{eq}(\boldsymbol{x}) = \frac{\int_\Omega \phi(\boldsymbol{x} - \boldsymbol{s})\varepsilon_{eq}(\boldsymbol{s})\, d\boldsymbol{s}}{\int_\Omega \phi(\boldsymbol{x} - \boldsymbol{s})\, d\boldsymbol{s}} \tag{7}$$

$\phi(\boldsymbol{x} - \boldsymbol{s})$ is the weight function defining the interaction between the considered point located at $\boldsymbol{x}$ and the neighboring points located at $\boldsymbol{s}$ inside the volume of the structure Ω. This formulation fulfills the requirement of nonalteration of a uniform field.

The most widely used nonlocal weight function is adopted as the Gauss distribution function:

$$\phi(\boldsymbol{x} - \boldsymbol{s}) = \exp\left(-\left(\frac{2\|\boldsymbol{x} - \boldsymbol{s}\|}{l_c}\right)^2\right) \tag{8}$$

where l_c is the internal length of the model and $\|\boldsymbol{x} - \boldsymbol{s}\|$ the distance between points located at $\boldsymbol{x}$ and $\boldsymbol{s}$. The characteristic size of the weighting domain directly depend on the characteristic length l_c.

The point located at $\boldsymbol{s}$ (distributing point) exerts an isotropic influence (Fig. 1a), except close to boundaries where the interaction domain is truncated. When considering a point at the level of the boundary, the number of distributing points with non-negligible influence on this point is halved. The term in the denominator in Eq. (7) is consequently halved as well, thus leading to a double amplitude of the interactions close to the boundary. As a result, an attraction of damage by the boundaries can be observed due to truncation of the interaction volume as illustrated by Krayani et al. (2009).

In Appendix A, we illustrate this unintended phenomenon of damage attraction by boundaries within the framework of the nonlocal integral method through studying the damage area under a Hopkinson test and analyzing how the proposed nonlocal method manages to describe interactions close to free boundaries.

Another issue identified is the treatment of FPZ at high damage levels. In Fig. 1b, a quarter of a plate with a central notch is shown; this specimen is submitted to a tension of equal magnitude in both directions. The circles indicated in the figure represent isovalues of the Gaussian function; these are similar at each point of the specimen and correspond to the influence of the point at the center of these circles. In the original nonlocal model, this point is able to influence a point on the other side of the crack since only the distance between them is considered in the model. From a physical standpoint however, this interaction should not exist. Since the presence of a FPZ or a fully developed crack, as well as a free boundary, modifies the loading on an RVE (Representative Volume Element) considered in the vicinity, the resulting redistribution of

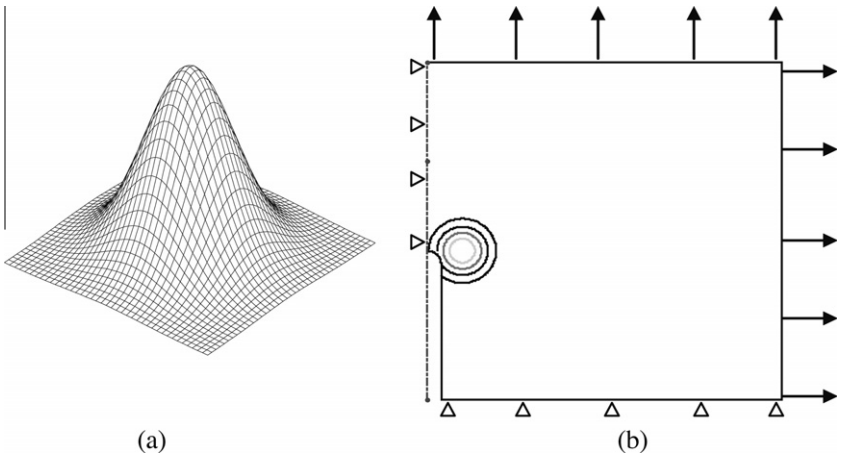

Fig. 1. Original nonlocal model: (a) influence of a distributing point, (b) isovalues of the influence of various points in the specimen.

this RVE at the origin of nonlocality had to be modified in order to reflect the evolution of interactions.

2.3. Nonlocal integral method based on stress state

As mentioned above, the truncation of interaction volume in the vicinity of the boundary leads to a double amplitude of the nonlocal terms in comparison with those in the bulk of the material. Based on micromechanical considerations, Pijaudier-Cabot and Dufour (2010) showed that nonlocality corresponds to a stress redistribution due to the presence of defects. In this framework, they demonstrated that nonlocalities should disappear in the vicinity of a boundary in the normal direction. As a consequence, they proposed a modification to the interaction domain (Krayani et al., 2009), whose shape is an ellipsoid with radius equal to the minimum of the internal length and the distance between the considered point and the boundary. The domain of interaction is oriented (i.e. isotropy is lost) yet does not evolve over time since only geometric aspects are being considered. The fully damaged area can be seen however as a new boundary surrounded by a damaged zone, which suggests that nonlocal interactions should vanish in the direction perpendicular to this new boundary.

According to our approach, the perspective for calculating nonlocal quantities is slightly different. *We no longer consider what a point located at* $\boldsymbol{x}$ *can receive, but instead what a point located at* $\boldsymbol{s}$ *can distribute*. The nonlocality is defined as a quantity given by each point located at $\boldsymbol{s}$ along its principal stress direction with an intensity depending on the level of principal stress. We introduce into the nonlocal regularization the two notions of directionality, as set forth by Pijaudier-Cabot and Dufour (2010) in the limited case of the vicinity of boundaries, and intensity variation, which depends on the state of loading in the structure. The stress field allows for a direct description of the presence of a free boundary and the development of fracture process zone, both of which lie at the origin of the modification of nonlocalities.

During the calculation, the evolution in interactions between points is considered through a single scalar ρ that, when multiplied by the characteristic length l_c (i.e. a length intrinsic to the material that can be correlated with aggregate size), defines the internal length of the model. This internal length rises from 0 for an unloaded material to l_c when reaching maximum tensile stress. It is important to note that this coefficient, which depends on the stress state of the distributed points, does not introduce any parameter into the model.

Let's denote $\boldsymbol{\sigma}_{prin}(\boldsymbol{s})$ as the stress state of the point located at $\boldsymbol{s}$, expressed in its principal frame. The vectors forming this frame are $\boldsymbol{u}_1(\boldsymbol{s})$, $\boldsymbol{u}_2(\boldsymbol{s})$, and $\boldsymbol{u}_3(\boldsymbol{s})$ with the associated principal stresses $\sigma_1(\boldsymbol{s})$, $\sigma_2(\boldsymbol{s})$ and $\sigma_3(\boldsymbol{s})$.

$$\boldsymbol{\sigma}_{prin}(\boldsymbol{s}) = \sum_{i=1}^{3} \sigma_i(\boldsymbol{s})(\boldsymbol{u}_i(\boldsymbol{s}) \otimes \boldsymbol{u}_i(\boldsymbol{s})) \tag{9}$$

where $\otimes$ is the tensor product. We define an ellipsoid centered at point $\boldsymbol{s}$, corresponding to a homothety of the original interaction domain, with a ratio $\left|\frac{\sigma_i(\boldsymbol{s})}{f_t}\right|$ along the principal stress direction $\boldsymbol{u}_i(\boldsymbol{s})$. f_t denotes the tensile strength of concrete.

The choice of f_t is motivated by the intention to describe the reduction in RVE during the cracking process. Its introduction leads to no modification of interactions at the tensile stress peak, in the direction associated with the maximum tensile stress, and thus allows regularizing direct mode I cracking. The characteristic length l_c associated with the material defines the maximum size of the interaction domain; hence, the internal length ρl_c of the stress-based nonlocal model cannot exceed this value. Consequently, the value of ρ needs to be limited to 1 under loading directions for which $|\sigma_i(\boldsymbol{s})|$ is greater than f_t.

By using the spherical coordinates (ρ, θ and ϕ), the following equation describes the ellipsoid associated with the stress state of the point located at $\boldsymbol{s}$ (Fig. 2).

$$\rho(\boldsymbol{x}, \boldsymbol{\sigma}_{prin}(\boldsymbol{s}))^2 = \frac{1}{f_t^2\left(\frac{\sin^2\varphi\cos^2\theta}{\sigma_1^2(\boldsymbol{s})} + \frac{\sin^2\varphi\sin^2\theta}{\sigma_2^2(\boldsymbol{s})} + \frac{\cos^2\varphi}{\sigma_3^2(\boldsymbol{s})}\right)} \tag{10}$$

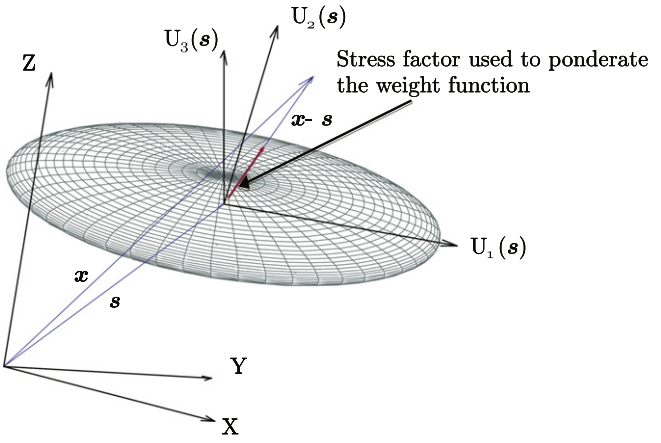

Fig. 2. Definition of the ρ coefficient indicating the influence of $\boldsymbol{s}$ on $\boldsymbol{x}$.

where θ is the angle between u_1 and the projection of $(\boldsymbol{x}-\boldsymbol{s})$ onto the plane defined by u_1 and u_2, and φ is the angle between u_3 and $(\boldsymbol{x}-\boldsymbol{s})$. In considering these angles, we obtain:

$$\cos\theta = \frac{\boldsymbol{u}_1 \cdot (\boldsymbol{u}_3 \wedge ((\boldsymbol{x}-\boldsymbol{s}) \wedge \boldsymbol{u}_3))}{\|\boldsymbol{u}_3 \wedge ((\boldsymbol{x}-\boldsymbol{s}) \wedge \boldsymbol{u}_3)\|} \quad \sin\theta = \frac{\boldsymbol{u}_2 \cdot (\boldsymbol{u}_3 \wedge ((\boldsymbol{x}-\boldsymbol{s}) \wedge \boldsymbol{u}_3))}{\|\boldsymbol{u}_3 \wedge ((\boldsymbol{x}-\boldsymbol{s}) \wedge \boldsymbol{u}_3)\|}$$
$$\cos\varphi = \frac{\boldsymbol{u}_3 \cdot (\boldsymbol{x}-\boldsymbol{s})}{\|\boldsymbol{x}-\boldsymbol{s}t\|} \quad \sin\varphi = \frac{(\boldsymbol{x}-\boldsymbol{s}) \cdot (\boldsymbol{u}_3 \wedge ((\boldsymbol{x}-\boldsymbol{s}) \wedge \boldsymbol{u}_3))}{\|(\boldsymbol{x}-\boldsymbol{s})\| \cdot \|\boldsymbol{u}_3 \wedge ((\boldsymbol{x}-\boldsymbol{s}) \wedge \boldsymbol{u}_3)\|} \tag{11}$$

where $\wedge$ is the vector product and "·" is the scalar product. The weight function now reads:

$$\phi(\boldsymbol{x}-\boldsymbol{s}) = \exp\left(-\left(\frac{2\|\boldsymbol{x}-\boldsymbol{s}\|}{l_c \rho(\boldsymbol{x}, \boldsymbol{\sigma}_{prin}(\boldsymbol{s}))}\right)^2\right) \tag{12}$$

with $\rho(\boldsymbol{x}, \boldsymbol{\sigma}_{prin}(\boldsymbol{s}))$ equal to the radial coordinate of the ellipsoid previously defined in the direction $(\boldsymbol{x}-\boldsymbol{s})$. According to the stress-based nonlocal model, the intensity of influence of a point at $\boldsymbol{s}$ on its vicinity depends on both the magnitude and direction of the principal stresses at $\boldsymbol{s}$. Fig. 3a provides the influence of the point located at $\boldsymbol{s}$ (distributing point) on its vicinity.

For the original nonlocal model, in the area where the redistribution domain is chopped off by the boundaries, the value of the term in the denominator depends on the distance to the edge (Eq. (7)). Therefore, the nonlocal kernel looses its symmetry nearby boundaries. The proposed formulation for the weight function leads to a non-symmetric nonlocal kernel in the whole domain (i.e. $\phi(\boldsymbol{x}-\boldsymbol{s}) \neq \phi(\boldsymbol{s}-\boldsymbol{x})$) since the stress states undergone by both the point located at $\boldsymbol{x}$ and the point located at $\boldsymbol{s}$ tend to differ most of the time. Described from a micromechanical perspective, several authors have revealed this non-symmetry of the nonlocal interactions. This was justified, on one hand, for ductile materials, by Voyiadjis and Abu Al-Rub (2005) considering dislocation densities and plastic strains and, on the other hand, for quasi-brittle materials, by Bažant (1994) or, more recently, Pijaudier-Cabot et al. (2004) looking at microcrack interactions.

Indeed, when considering interactions between circular voids using the analytical method developed by Kachanov (1987) and Pijaudier-Cabot et al. (2004) indicate that the state at the point located at $\boldsymbol{x}$ is the sum of a local quantity at $\boldsymbol{x}$ under remote loading σ_∞ and a nonlocal quantity stemming from a stress redistribution, due to the presence of microcracks, of the surrounding points at $\boldsymbol{s}$ under the remote loading (see Eq. (13)).

$$\sigma(\boldsymbol{x}) = \sigma_\infty(\boldsymbol{x}) + \sum l_{\boldsymbol{xs}}^2 \sigma_\infty(\boldsymbol{s}) \tag{13}$$

where $l_{\boldsymbol{xs}}$ is an interaction factor derived from the Eshelby solution to the perturbation stress field due to a circular inclusion loaded by internal pressure. This factor is proportional to the distance between $\boldsymbol{x}$ and $\boldsymbol{s}$ and to the radius of the circular void $r_\iota(\boldsymbol{s})$ (which makes it somewhat proportional to crack size) at $\boldsymbol{s}$. Since the radius of a circular void may differ for each point ($r_\iota(\boldsymbol{s}) \neq r_\iota(\boldsymbol{x})$), the interaction factors $l_{\boldsymbol{xs}}$ (i.e. the influence of $\boldsymbol{s}$ on $\boldsymbol{x}$) and $l_{\boldsymbol{xs}}$ (influence of $\boldsymbol{x}$ on $\boldsymbol{s}$) may also differ, leading thus to a non-symmetry of the nonlocal kernel. In conclusion, the newly proposed interaction kernel is non-symmetric as the original one along the boundaries and as all the recent improved propositions based on micromechanical considerations.

With the stress-based nonlocal method proposed herein, we are able to retrieve the specific shape of the flat ellipsoid proposed by Krayani et al. (2009) in the case of a free boundary. The following condition can thus be derived for the stress tensor: $\boldsymbol{\sigma}_{prin}(\boldsymbol{s}) \cdot \boldsymbol{n} = \boldsymbol{0}$ with $\boldsymbol{n}$ being the normal vector to the free boundary. As a result, the points in this area are local in the normal direction.

For purpose of illustration, we have studied a plate with a central notch under isotropic biaxial traction. In Fig. 3b, the point C is not influenced by the notch, which is why the isovalues are close to being circular. For the point B, in the vicinity of the crack tip, the stress state is highly disturbed and oriented, leading to ellipses for the isovalues. The point A is shielded by the crack and hence undergone only a very low stress state, a situation that exerts no influence on the surrounding points, as would be expected from micromechanics.

2.4. Numerical implementation

2.4.1. Computation of the interaction weights for the original nonlocal model

The general algorithm of the original nonlocal method has been described in details by Pegon and Anthoine (1997). A fixed connectivity matrix is initially created by defining a list of interacting neighboring elements j for each element i. The interaction domain computed for each point is reduced in order to maintain the band structure of the secant operator during the calculation. A geometric criterion is thus considered by retaining only those elements j for which the distance between one of their nodes and a node of the element i is less than $1.5 \times l_c$. This limit corresponds to an interaction weight ϕ of 1% for a Gaussian distribution. It leads to a bandwidth of the secant operator proportional to l_c. Consequently, the higher the internal length is, the wider the bandwidth will be and the longer the computational time will be. During the initial step, in order to limit data storage requirements, the weighting is not stored. Only Boolean values listing the connected elements are actually stored. This description of the connected elements is performed once at the beginning and accounts thus for a fixed computational cost.

During the calculation, the nonlocal regularization is performed just after evaluating the equivalent strain ε_{eq}. The distance to each

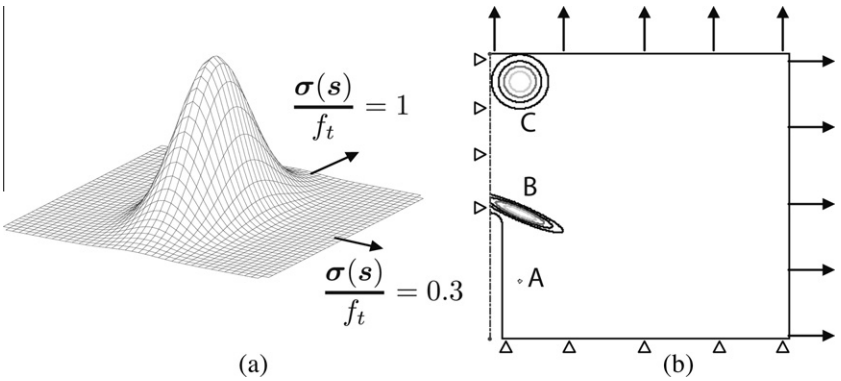

Fig. 3. Stress-based nonlocal model: (a) influence of a distributing point, (b) isovalues of the influence of various points in the specimen.

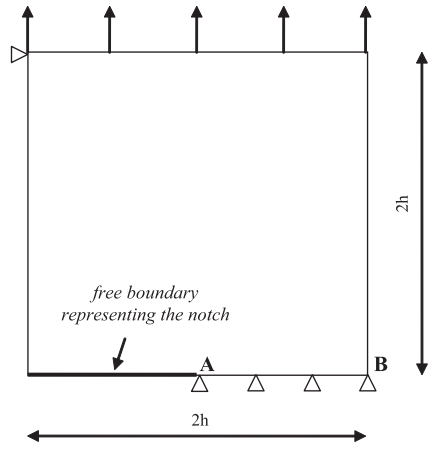

Fig. 4. Compact tension specimen (CTS).

surrounding Gauss points is then used to compute the weight function between connected points.

2.4.2. Modifications for the stress-based nonlocal model

The same procedure used for the original nonlocal method is selected for the stress-based nonlocal method. Since the coefficient ρ remains lower or equal to 1, the interaction domain for the stress-based nonlocal method is always included within the domain for the original nonlocal method, meaning that the connectivity matrix computation, performed at the initial step, is unaffected by the new regularization method and retained for the stress-based nonlocal approach. During the calculation, in addition to the distance to each surrounding Gauss points, the stress state of each Gauss points is collected in order to compute the weight function of the stress based nonlocal method. In order to retain an explicit resolution of the constitutive law, interactions have been computed using the stress state of the previous converged step.

In the definition of ρ, the direction between the point at $\boldsymbol{x}$ and the point at $\boldsymbol{s}$ needs to be calculated. For the specific case in which these two points are merged, the coefficient ρ is not defined since no direction can be computed. Nevertheless, by considering a non-zero value for ρ and with a distance $\|\boldsymbol{x}-\boldsymbol{s}\|$ equal to zero, the weight for the point located at $\boldsymbol{x}$ is equal to 1; this corresponds to the local part of the nonlocal equivalent strain.

2.4.3. Definition of the minimum internal length

Under a uniaxial load, the ellipsoid degenerates into a line with a zero volume. With no minimum size, this specific case yields no interaction, though a point can be exposed to a relatively high stress magnitude in one direction. A minimum value of ρ is therefore prescribed to avoid difficulties with zero stress in certain directions. The minimum value of the internal length ρl_c is set equal to the characteristic local size of the element ($\sqrt{area}$, in 2D and $\sqrt[3]{volume}$, in 3D) and then initially computed for each element. For a point under high uniaxial stress state, this choice serves to influence the vicinity along the principal stress directions over a domain, even though it remains local in the zero-stress direction. On the other hand, this value also ensures a minimum size of the interaction domain of less than a single element at complete failure in order to avoid interactions between points across a macrocrack. Appendix B analyzes the influence of this minimum value. Such a rather arbitrary choice has been studied through testing of a 2D bar under tension with an unstructured mesh.

2.4.4. Treatment of the symmetry

For the original nonlocal method, symmetry conditions are treated by constructing a mirror image of Gauss points that respect the symmetry. Nonlocal averaging is then performed over the entire domain of interactions, including newly-created points. For the stress-based nonlocal method, the same procedure is implemented, using in addition, the symmetric stress state associated with the newly-created points in order to compute the weight.

2.4.5. Choice of the solver for the operator

In terms of computational cost, the stress-based nonlocal method follows the same algorithm as the original nonlocal method. Due to truncation of the interaction volume close to the boundary, introducing the original nonlocal regularization leads to a non-symmetric operator and thus precludes the use of algorithms when considering the symmetry of the secant operator. For the stress-based nonlocal model, due to non-reciprocity of the interactions, given that the stress state tends to be different for each Gauss point most of the time, the consistent stiffness matrix becomes non-symmetric even in the bulk part of the model.

Consequently, only the calculation of coefficient ρ, at each step of the calculation, affects the general algorithm of the stress based-nonlocal method compared to the original one.

All the calculations presented in this paper have been executed using the finite element code Cast3M developed by the C.E.A. (French Nuclear Agency) (Verpeaux et al., 1988), in which the stress-based nonlocal method has been implemented.

3. Failure in mode I

3.1. Initiation phase

Mode I damage initiation is analyzed by means of the compact tension specimen, with a preexisting crack of length h = 0.0005 m, as shown in Fig. 4. This test, originally conducted by Simone et al.

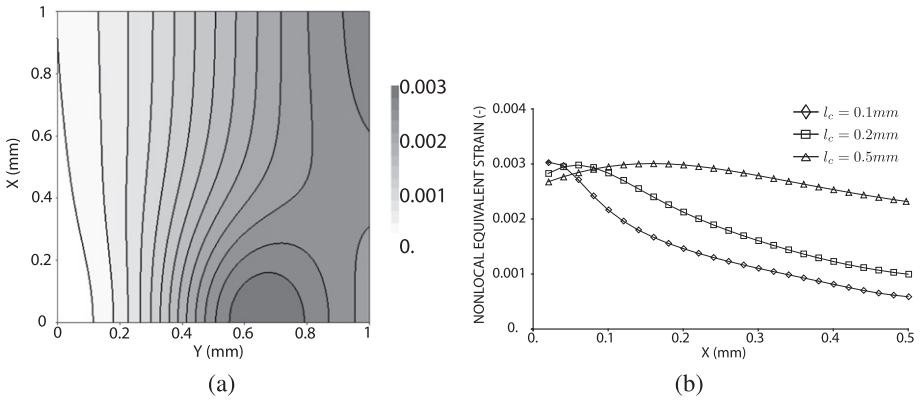

Fig. 5. CTS: original nonlocal model, (a) contour plot of the nonlocal equivalent strain; and, (b) evolution of the nonlocal equivalent strain along AB.

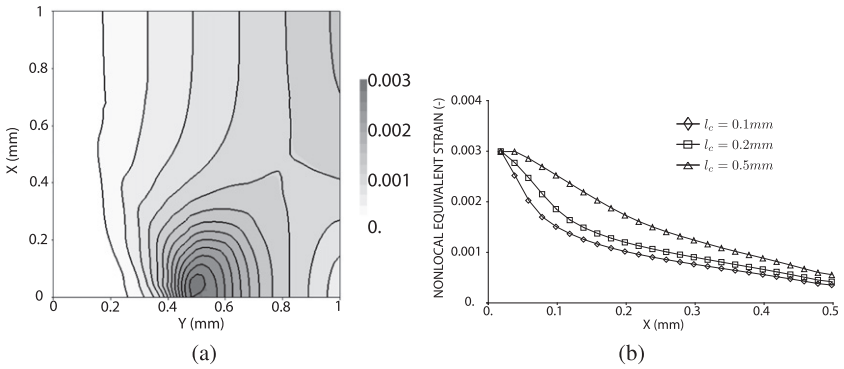

Fig. 6. CTS: stress-based nonlocal model, (a) contour plot of the nonlocal equivalent strain; and, (b) evolution of the nonlocal equivalent strain along AB.

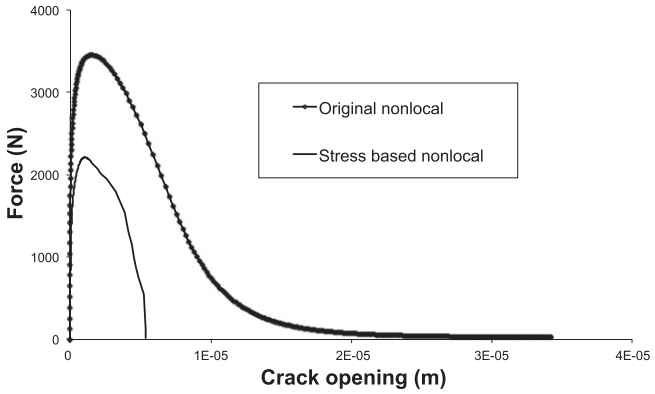

Fig. 7. Force vs. crack opening for both nonlocal methods.

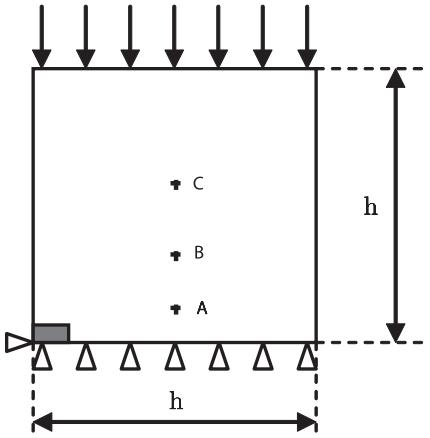

Fig. 9. Geometry and boundary conditions for the specimen under compression (h = 60 mm; weak area: $h/10 \times h/20$).

(2004), in order to study the location of damage initiation for the regularized damage models has been reproduced with the stress-based nonlocal method. Since our interest herein lies in describing crack initiation and corroborating the work accomplished by Simone et al., the notch has been described geometrically. Thanks to symmetry, only half of the specimen needed to be meshed.

The following parameters for the material are used for the analysis: E = 1000 MPa and $\nu = 0.2$. Various characteristic lengths for the nonlocal integral method were introduced for the calculations, as a means of determining the influence on location of the maximum equivalent strain: $l_c = 0.0001$, 0.0002 and 0.0005 m.

We verified the location of the damage initiation is not influenced by the value of the Poisson's ratio for both the original nonlocal model and the stress-based nonlocal model. With a more realistic value for a concrete-like material of the Poisson's ratio ($\nu = 0.2$), we retrieve exactly the same position for the damage initiation than in Simone et al. (2004) with $\nu = 0$. The equivalent strain as defined by de Vree (Eq. (3)) was calculated from the strain field obtained under an imposed displacement. The nonlocal equivalent strain could then be computed (Eq. (7)); the field value is plotted in Fig. 5a. As pointed out by Simone et al. (2004), it can be observed that the maximum value is reached ahead of the notch tip using either gradient or nonlocal regularization methods. Furthermore, Fig. 5b shows the value of the nonlocal equivalent strain projected

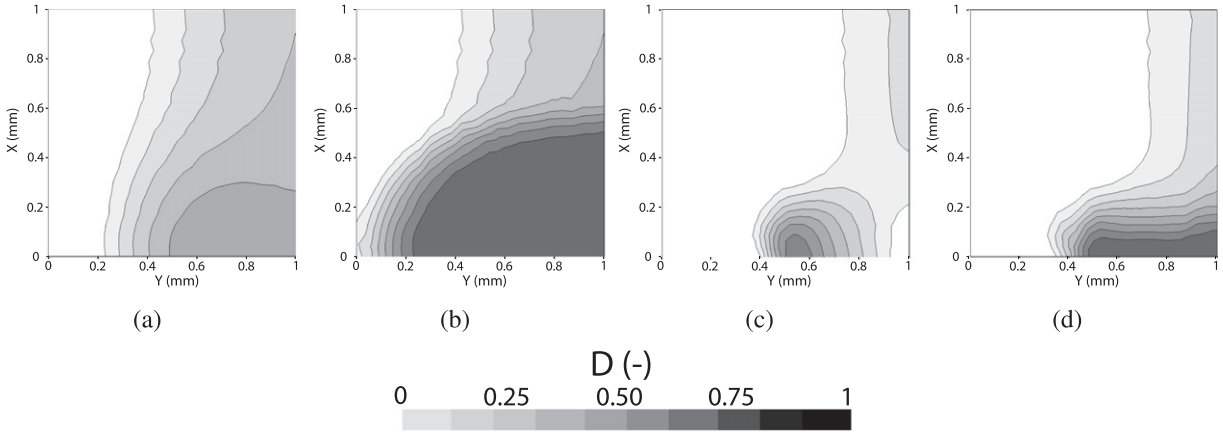

Fig. 8. CTS: Damage field at peak force and at failure ((a) and (b): original nonlocal and (c) and (d): stress-based nonlocal).

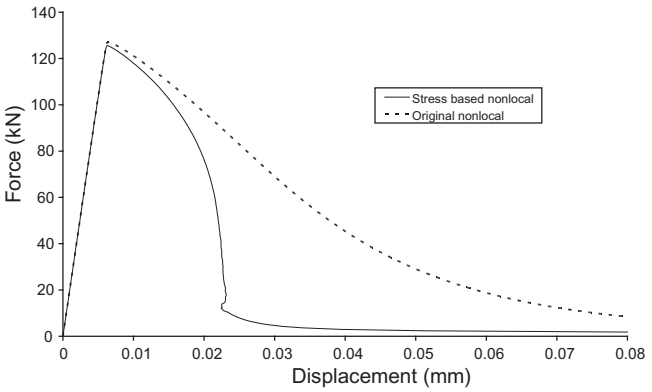

Fig. 10. Global behavior of the compression specimen for both regularization methods.

along the line *AB* in front of the crack. Let's note that the shift is proportional to the internal length of the nonlocal method as also mentioned in the previously cited work. In the original version the interaction domain extends over the shadow zone of the notch where strains are close to zero. Since the nonlocal equivalent strain is a weighted summation, it proportionally reduces the impact of the singular strain. Since the strain gradient is smaller in front of the notch than at the back, the nonlocal equivalent strain is shifted ahead of the notch front.

It is worth noting however that for the same test with the stress-based nonlocal method, this shift is null regardless of the characteristic length l_c (Fig. 6a and b). The points lying in the shadow of the notch exposed to a small local equivalent strain also lie in a low stress state. Consequently, their influence on the vicinity is hardly nonexistent. This important result displays the capability of the stress-based nonlocal method to correctly locate the initiation of material nonlinearities in a mode I problem with a preexisting crack. This issue is a key to the size effect analysis.

3.2. Propagation of damage

To illustrate the difference between both methods, the calculation has been performed up to failure. The following parameters have been used: $E = 1000$ MPa, $\nu = 0.2$, $l_c = 0.56$ mm, $\varepsilon_{D_0} = 0.003$, $\alpha = 0.99$, $\beta = 100$ and $k = 10$. In Fig. 7, the crack opening has been computed according to the method proposed by Dufour et al. (2008). The point of the crack considered to compute the crack opening is the one just in front of the notch tip. With the same set of parameters, it can be observed, damage initiates earlier with the stress based nonlocal model since the interaction domain is smaller and the strain field is singular. Furthermore, the peak force obtained is smaller with the stress based nonlocal method. Regarding the damage field, with the original nonlocal model, the shift in damage from the crack tip can still be observed at the peak (Fig. 8(a)). This observation reinforces the previous remark regarding size effect since the peak force is being directly used to for these analyses.

After damage initiation, it can be observed that the stress-based nonlocal model dissipates less energy than the original method. Moreover, during the post-peak behavior, one can see that the damage returns along the notch with the original nonlocal model. This non-physical description of damage evolution has not been obtained with the stress-based nonlocal given that the stress state avoids interactions with points in back of the crack tip.

4. Damage characterization in shear band problems

Shear banding is a classical collapse mechanism undergone in many engineering problems relative to geomaterials under

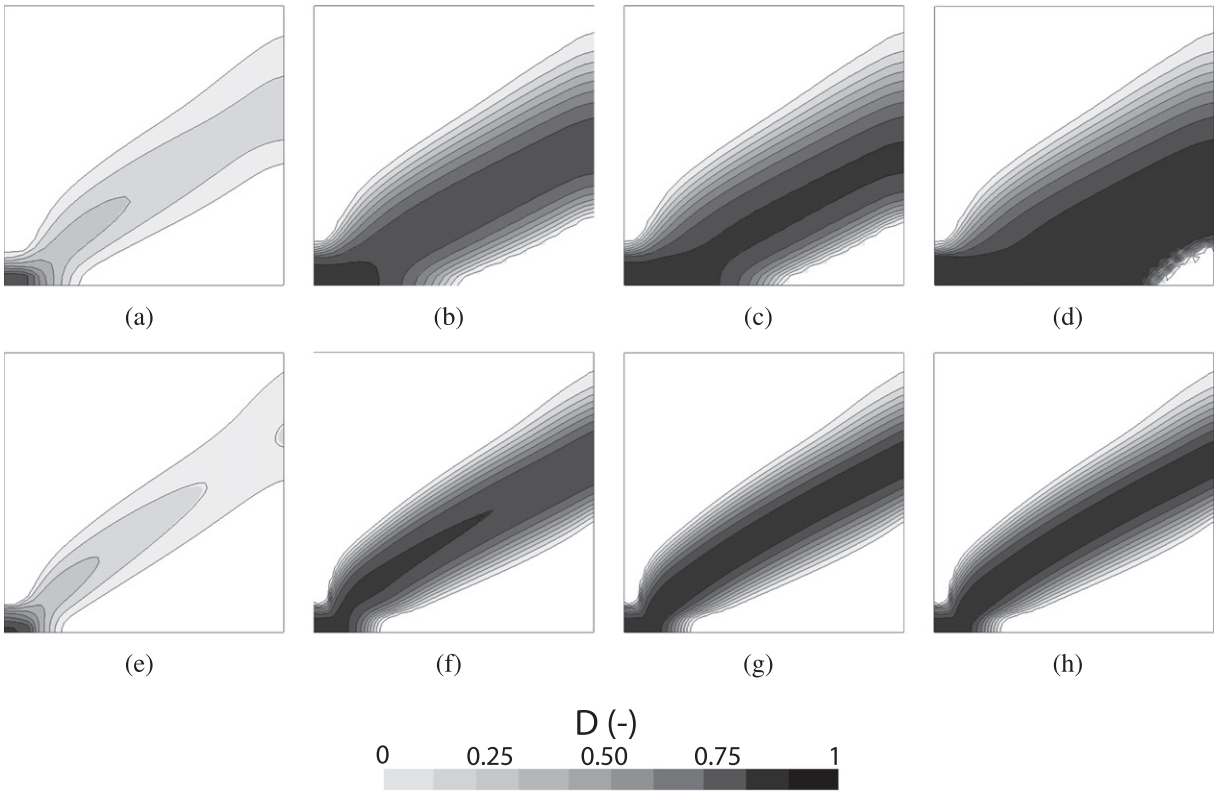

Fig. 11. Shear band evolution: Contour plots of the damage field with the original nonlocal method ((a)–(d)) and the stress based nonlocal method ((e)–(h)). Displacement: 0.0065 mm; 0.015 mm; 0.02 mm; and, 0.08 mm.

complex loading. Among the various case studies, we can highlight some specimens under compressive loading that exhibit shear bands. The main objective of the current analysis is to assess the numerical results obtained in a specific problem involving shear bands with both the original and stress-based nonlocal regularization techniques. Simone et al. (2004) have shown the wrong prediction of propagation for a shear band induced by a gradient-enhanced continuum damage model.

4.1. Case study

A specimen under compressive loading has been studied to illustrate shear band problems (Fig. 9). To describe the material, the following parameters for the exponential evolution law presented in the first part (Eq. (6)) (Peerlings et al., 1998) and von Mises equivalent strain (Eq. (3)) (de Vree et al., 1995) have been used: $E = 20,000$ MPa, $\nu = 0.2$, $l_c = 2.83$ mm, $\varepsilon_{D_0} = 0.0001$, $\alpha = 0.99$, $\beta = 300$ and $k = 1$.

The brittle behavior associated to the stress–strain law typically induces snap-back responses, thus requiring arc-length control in order to solve the nonlinear systems of equations. Furthermore, with the stress-based nonlocal regularization, damage tends to localize in a narrower band than with the original nonlocal model. As stated by Rodríguez-Ferran and Huerta (2000), standard arc-length techniques, such as spherical or cylindrical formulations (Crisfield, 1991), are not suitable in this case since they provide a measure of the increment of the solution that is too "global" in contrast with the localized nature of the problem (Geers, 1999). Alternatively, more "local" definitions of the arc-length parameter s are needed, such as the maximum strain increment (Pegon and Anthoine, 1997; Rodríguez-Ferran and Huerta, 2000).

$$\Delta s = \max |\Delta \varepsilon_{ij}| \tag{14}$$

For this test, the loading has been applied via an arc-length control. In order to initiate damage in this homogeneous model, a weak area is introduced with a lower damage threshold ($\varepsilon_{D_0} = 0.00005$).

Fig. 10 exhibits the global behavior of the specimen under compressive loading for both the original and stress-based nonlocal regularization techniques with an element size equal to 0.001 m. Fig. 11a–d show the damage field at different steps of the calculation using the original nonlocal regularization technique. After damage initiation, we can observe a gradual shift in the shear band along the boundary, as indicated in Simone et al. (2004). The internal length value influences the shift observed along the boundary.

Fig. 11e–h present the damage field at various steps of the calculation with the stress-based nonlocal regularization technique. The stress state undergone by the points with highest equivalent strain (main stress intensity along the loading axis) avoids a redistribution along the boundary and thus eliminates an incorrect damage propagation. In addition, the highest damage points are concentrated over a confined area that may be viewed as the sliding plane between the two parts of the specimen.

Fig. 12 provides the evolution in the parameter $\rho(\boldsymbol{x}, \boldsymbol{\sigma}_{prin}(\boldsymbol{s}))$ at different steps of the calculation (displacement: 0.006 mm, 0.016 mm, 0.022 mm for three distinct locations: Point A (0.03; 0.005), Point B (0.03; 0.02) and Point C (0.03; 0.04)). As stated

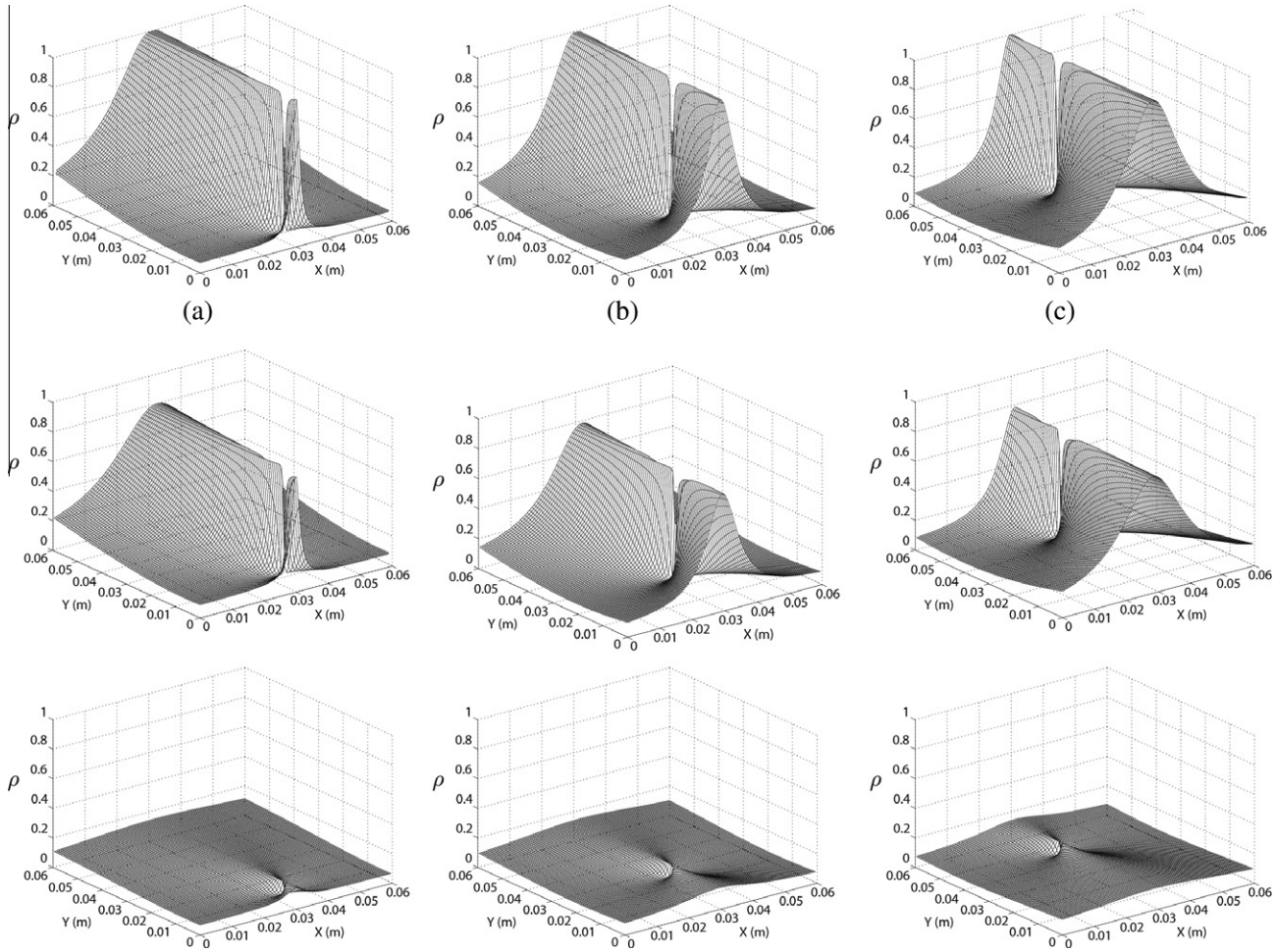

Fig. 12. Evolution of $\rho(\boldsymbol{x}, \boldsymbol{\sigma}_{prin}(\boldsymbol{s}))$ during the loading. (a) Point A; (b) Point B; and, (c) Point C.

in Section 2.4, at **s** to be equal **x**, ρ is not defined and the weight function is equal to one, which explains the hole at the location of **x** in Fig. 12. The first step considered consists of representing the ρ field close to the peak force, thus making it possible to observe a maximum value for ρ along the loading direction. Since the loading is unidirectional, the redistribution is highly oriented with no influence in the x-direction. When damage propagates inside the specimen, stress intensity decreases as does the influence of points on their vicinity. At complete failure, the ρ field for all three points tends to zero. The points behave locally with no quantity being redistributed.

The objectivity (Fig. 13) of this model is also verified using various mesh sizes (0.0015 and 0.00075 m), in addition to an unstructured mesh (with an average mesh size: 0.001 m). The global behavior (force vs. displacement curves) and local behavior (location, orientation and size of the shear band) are identical for all cases. In Fig. 13a, we observe at complete failure (i.e. the shear band has reached the opposite side of the specimen) a small corner in the global response. At this step, the energy dissipation is almost completed. Consequently, after this step, the displacement increased with no discernible evolution in the force which is close to zero, leading thus to a change of direction in the evolution of the force vs. displacement curve. Close to complete failure, since the maximum damage tends to be localized in one element with the stress based nonlocal method, the ultimate variation of dissipated energy depends on the size of the element. Consequently, we observe a small discrepancy at failure between the different mesh size without affecting the global amount of dissipated energy. However, as the element size tends to an infinitely small value, this variation between two different meshes becomes insignificant.

The influence of plane stress or plane strain condition is discernible in Fig. 14. The damage field shown is the one obtained for an imposed displacement of 0.08 mm. In accordance with Rizzi et al. (1995) for the scalar damage model, the only noticeable change between the plane strain conditions and the plane stress

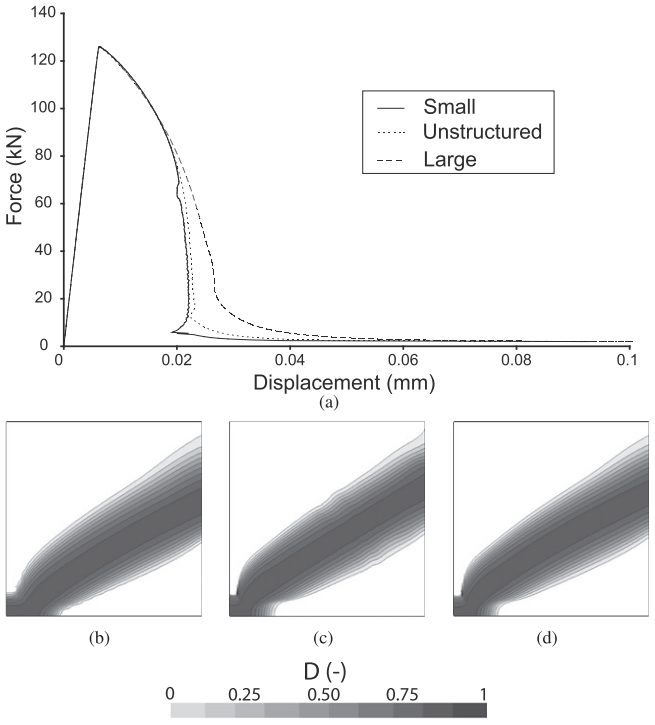

Fig. 13. (a) Global behavior. Damage field: (b) large mesh; (c) unstructured mesh; and, (d) small mesh.

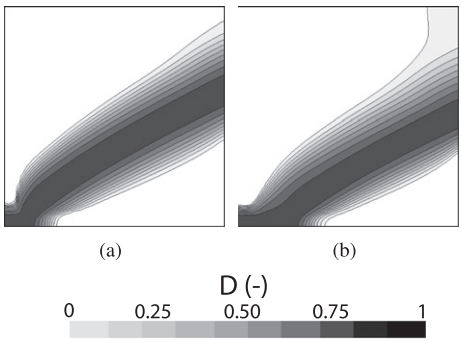

Fig. 14. Damage field: (a) plane strain condition; and, (b) plane stress condition.

conditions with the stress-based nonlocal model is an altered inclination of the shear band.

This test has demonstrated the capability of the stress-based nonlocal model to better reproduce both damage propagation and shear band localization.

5. Conclusions

In this paper, we have proposed a modification to the nonlocal integral model in order to adapt the regularization close to the free boundaries as well as during the cracking process. The stress state of each point is used during the calculation to create an evolution of the interaction between points. Each point interacts with its vicinity as a function of the intensity and direction of its principal stresses. This modification has been presented for a 3D case and has led to the retrieval of results relative to the boundary effects given in a previous article by the 2nd author, yet without any specific treatment of boundaries.

The stress-based nonlocal approach yields a better solution for modeling damage initiation and propagation of the localization zone. Through two examples, we have shown that the proposed approach is perfectly capable of locating damage initiation, which is poorly estimated using any of the other regularization techniques. This work has also concluded that the damage area does not follow the boundary during its propagation. The stress-based nonlocal method relies on reducing the principal stress perpendicular to the crack. Initial simulations performed on mode II have shown an improvement; however, further investigations are underway for complex failure mode.

All these improvements are introduced with no additional parameters, since this would be difficult to calibrate. Moreover, this method can be easily implemented in any FE code that already includes a nonlocal integral approach.

In future work, a loaded interface between two materials and loaded boundaries will be investigated. Such an investigation will be of great benefit for structural analysis with the interaction between a concrete crack and rebar.

Acknowledgements

The authors gratefully acknowledge the financial support received from France's National Research Agency through the Agency's sustainable cities program. (contract reference: VD08_323065).

Appendix A. Analysis of boundary effect: spalling test

In order to study the results given by the original and stress-based nonlocal methods close to a free boundary, let's start by considering a one-dimensional dynamic tension test (i.e. the split

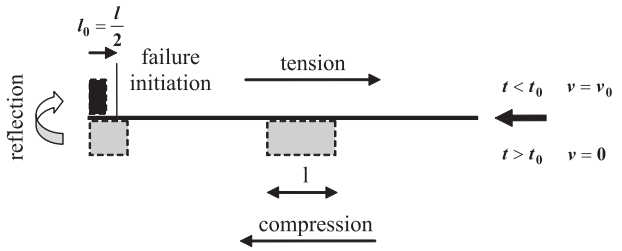

Fig. A.15. Split Hopkinson bar test.

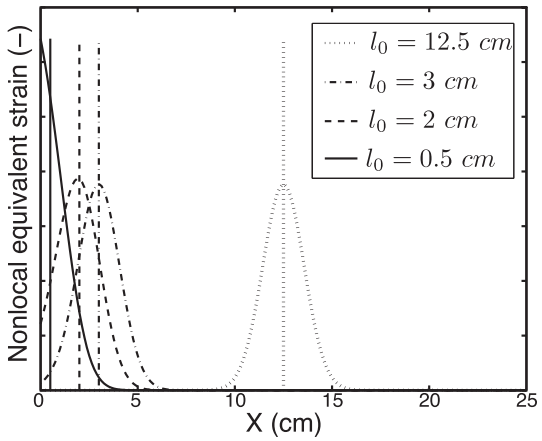

Fig. A.16. Attraction of the maximum nonlocal equivalent strain by the boundary. Influence of the location l_0 of the tensile signal appearance.

Hopkinson bar test), as shown in Fig. A.15. This example allows to initiating failure close to a free boundary. A square compression signal is generated within the bar. Upon reflection at the end of the bar, the compression signal transforms into a tensile signal that gets added to the incoming compression. If the absolute amplitude of the compression signal exceeds the tensile strength, then failure is initiated at a distance from the boundary equal to half the signal length. Depending on the compression signal duration, it is possible to initiate failure in the material at any location, either near the boundary or far from it. Let's first study this problem analytically in order to illustrate the unintended attraction of damage by the boundary using the original nonlocal model. Afterwards, a numerical analysis will be performed to compare the capability of both nonlocal methods in describing failure close to the free boundary.

A.1. Analytical analysis

From an analytical perspective, let's study the nonlocal equivalent strain field regularized with the original nonlocal model at the time when the tensile signal first appears. Let us assume the positive part of the strain field can be represented by a Dirac function δ:

$$\varepsilon_x(x) = \varepsilon_0 \delta(x - l_0) \tag{A.1}$$

with ε_0, the amplitude of the signal and l_0 the location of the Dirac. The nonlocal equivalent strain is then computed according to Eq. (7):

$$\overline{\varepsilon_{eq}}(x) = \frac{\varepsilon_0 \phi(x - l_0)}{\int_0^{\ell} \phi(x - s)\, ds} \tag{A.2}$$

with ϕ the Gaussian function defined in Eq. (8). To illustrate the phenomenon of attraction by the boundary, let's consider different locations l_0 for the first appearance of the tensile signal. The bar length ℓ is set equal to 25 cm. The characteristic length of the original nonlocal l_c is 3 cm. Fig. A.16 shows the nonlocal equivalent strain field along the bar for various values of l_0. In the middle, the local and the nonlocal maximum equivalent strain are placed at the same location. A shift between the maximum local equivalent strain and the maximum nonlocal equivalent strain can be observed close to the boundary. When l_0 becomes lower than the value of the internal length l_c of the original nonlocal model,then the maximum is attracted by the boundary due to the truncated interaction volume, and this situation therefore leads to an incorrect damage initiation.

A.2. Numerical analysis

The parameters used in this example are: mass density ρ = 1 kg/m^3, Young's modulus E = 1 MPa and the velocity boundary condition v_0 = 3.5 mm/s applied at the right bar end. The other model parameters are listed as: α = 1; β = 2; $\varepsilon_{D_0} = 1$ and the characteristic length l_c is 3 cm (no damage is present in compression). A fixed mesh of 250 constant strain elements has been adopted. Time integration is performed according to an explicit, central difference scheme. The signal length is calculated as $l = t_0 c$ and its amplitude is $\frac{v_0}{c}$ where c is $\sqrt{E/\rho}$.

Let's study the evolution of damage from initiation until failure with both nonlocal formulations. The chosen length l of the signal leads to a damage initiation close to the boundary at a distance of 1.5 cm (the signal length is 3 cm).

According to the original formulation (Fig. A.17(a)), damage is maximum at the bar extremity once it has sufficiently developed.

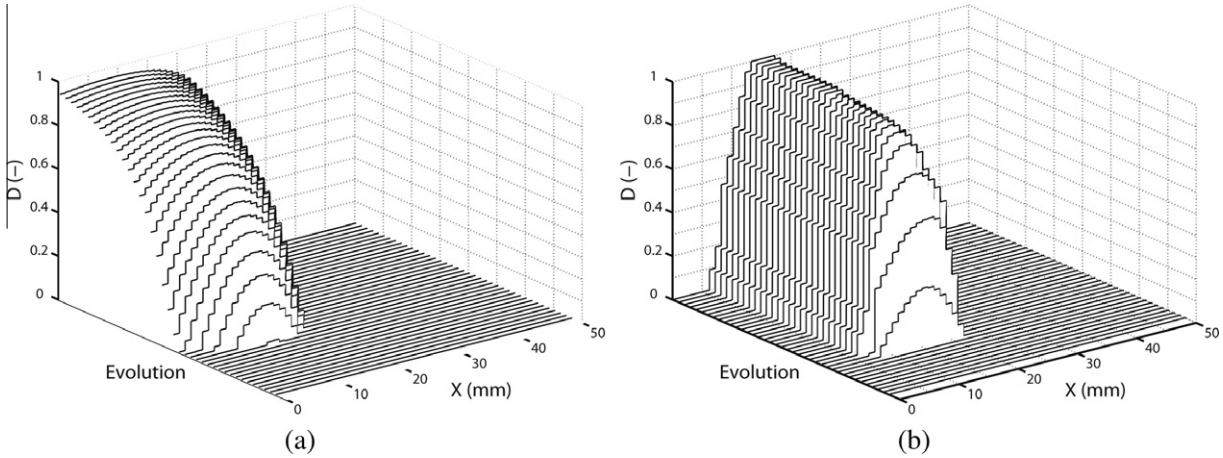

Fig. A.17. Damage profile when damage initiates nearby the extremity of the bar: (a) original nonlocal model; and, (b) stress-based nonlocal model.

We can observe a damage attraction by the boundary with a gradual shift of the maximum. According to the stress-based formulation (Fig. A.17(b)), damage is maximum inside the bar, where tension is initiated and where the extremity displays no damage. Let's now define the thickness of the spall as the distance between the left-hand side extremity of the bar and the closest point at which damage is equal to 1 (i.e. complete failure). This thickness is infinitesimally small according to the original nonlocal approach because maximum damage occurs at the bar extremity. Consequently, it is impossible to obtain a spall on the order of the characteristic length of the material or less using the original nonlocal formulation. Damage initially develops with a maximum inside the bar, but as it expands, the maximum damage is attracted towards the bar extremity. In contrast, such is not the case with the stress-based nonlocal formulation mainly because interactions decrease near the bar extremity as stresses decrease with increased damage.

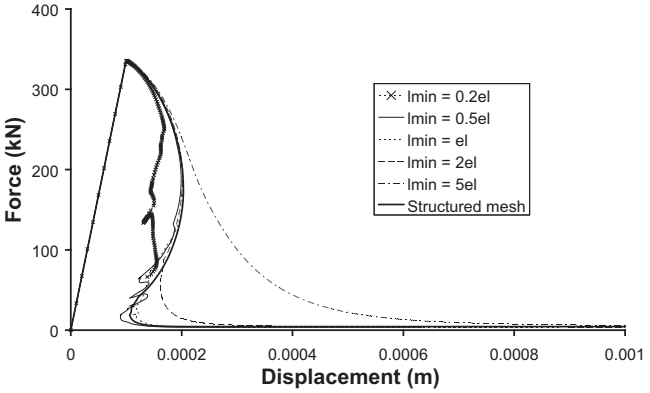

Fig. B.19. Comparison of the global response with different minimum values imposed for ρ.

Appendix B. Influence of the minimum value of ρ

The influence of the prescribed minimum value for coefficient ρ is studied with a simple example of a 2D bar under tension and a 1D loading (i.e. no Poisson's effect). In this application, due to zero stress in the Y-direction, a minimum value of ρ is prescribed during the loading.

With a regular mesh describing the bar, we obtain an alignment of Gauss points parallel to the loading direction. As a result, the interactions between nearby points are maintained even with a very small prescribed value for ρ. Let's consider this solution as the reference and focus on the influence of the minimum value of ρ with an unstructured mesh (Fig. B.18).

The bar is 1 m long and 0.1 m high; it is fixed at one end. The following parameters have been set for the damage model describing concrete (see Eq. (6)): $E_b = 33.7$ GPa, $\alpha = 0.99$, $\nu = 0$, $\beta = 1000$ and $l_c = 0.18$ m.

Five prescribed minimum values for ρ have been tested with the unstructured mesh: $\frac{5d_{min}}{l_c}$, $\frac{2d_{min}}{l_c}$, $\frac{d_{min}}{l_c}$, $\frac{0.5d_{min}}{l_c}$ and $\frac{0.2d_{min}}{l_c}$ with d_{min} being a characteristic size of the element ($\sqrt{area}$).

The loading has been applied via an arc-length control. The mesh is composed of bilinear quadrilateral elements for the reference solution and constant-strain triangular elements for the unstructured mesh. The central band of elements is weakened by a lower Young's modulus ($E_{b_{weak}} = 31$ GPa) in order to initiate damage in the bar. Fig. B.19 shows the evolution in force vs. displacement for the various minimum values of ρ. The response obtained is similar at the beginning of the post-peak behavior for the minimum values greater or equal to $\frac{0.5d_{min}}{l_c}$. Once the minimum value of ρ has been reached however, the size of the localization area is imposed. With a value above d_{min}, the maximum damage can no longer be localized within a bandwidth of an element at complete failure, and we obtain greater energy dissipation, which in turn leads to differences relative to the global response. For $\frac{0.5d_{min}}{l_c}$, we observe a response similar to the reference solution. In this case however, some points behave locally even at high stress since they lie outside the area of influence of neighboring points. This tendency is amplified in the unstructured mesh, as the minimum imposed value tends to decrease. When the width of the interaction domain becomes too small, the number of integration points influenced heavily depends on their alignment. For the unstructured mesh, this situation leads to a non-physical response with oscillations.

Compared to the reference solution, a minimum value of ρ equal to $\frac{d_{min}}{l_c}$ allows localizing maximum damage within a bandwidth of one element without loosing the nonlocal interactions between close points at high loading levels. This value has been selected for the range of tests proposed in this paper.

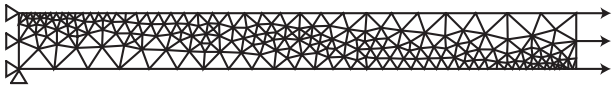

Fig. B.18. Bar under tension. Unstructured mesh.

References

Bažant, Z., 1991. Why continuum damage is nonlocal: micromechanics arguments. Journal of Engineering Mechanics ASCE 117 (5), 1070–1087.

Bažant, Z.P., 1994. Nonlocal damage theory based on micromechanics of crack interactions. Journal of Engineering Mechanics 120, 593–617.

Bažant, Z.P., Jirasek, M., 2002. Nonlocal integral formulations for plasticity and damage: survey of progress. Journal of Engineering Mechanics 128, 1119–1149.

Bažant, Z.P., Le, J.-L., Hoover, C.G., 2010. Nonlocal boundary layer (nbl) model: overcoming boundary condition problems in strength statistics and fracture analysis of quasibrittle materials. In: 7th International Conference on Fracture Mechanics of Concrete and Concrete Structures (FraMCoS-7).

Crisfield, M.A., 1991. Non-linear Finite Element Analysis of Solids and Structures. Wiley, Chichester, vol. 1.

Desmorat, R., Gatuingt, F., 2007. Introduction of an internal time in nonlocal integral theories, internal report LMT-Cachan, number 268, year 2007, ENS Cachan/CNRS/Université Paris 6/PRES Universud Paris. <http://hal.archives-ouvertes.fr/hal-00200898/en/>.

Desmorat, R., Gatuingt, F., Ragueneau, F., 2010. Nonstandard thermodynamics framework for robust computations with induced anisotropic damage. International Journal of Damage Mechanics 19 (1), 53–73.

de Vree, J., Brekelmans, W., Van, A., 1995. Comparison of nonlocal approaches in continuum damage mechanics. Computers and Structures 55, 581–588.

Dufour, F., Pijaudier-Cabot, G., Choinska, M., Huerta, A., 2008. Extraction of a crack opening from a continuous approach using regularized damage models. Computers and Concrete 5 (4), 375–388.

Eringen, A.C., Speziale, C.G., Kim, B.S., 1977. Crack-tip problem in non-local elasticity. Journal of the Mechanics and Physics of Solids 25, 255–339.

Geers, M., 1999. A unification of path following techniques for nonlinear finite element analyses. In: Wunderlich, W., München, G. (Eds.), Conf. on Comp. Mech. Vol. On CD-Rom.

Geers, M.G.D., de Borst, R., Brekelmans, W.A.M., Peerlings, R.H.J., 1998. Strain-based transient-gradient damage model for failure analyses. Computer Methods in Applied Mechanics and Engineering 160 (1–2), 133–153.

Jirasek, M., Rolshoven, S., Grassl, P., 2004. Size effect on fracture energy induced by non-locality. International Journal for Numerical and Analytical Methods in Geomechanics 28 (7–8), 653–670.

Kachanov, M., 1987. Elastic solids with many cracks-a simple method of analysis. International Journal of Solids and Structures 23, 23–43.

Krayani, A., Pijaudier-Cabot, G., Dufour, F., 2009. Boundary effect on weight function in non-local damage model. Engineering Fracture Mechanics 76, 2217–2231.

Peerlings, R.H.J., de Borst, R., Brekelmans, W.A.M., de Vree, J.H.P., 1996. Gradient enhanced damage for quasi-brittle materials. International Journal for Numerical Methods in Engineering 39, 937–953.

Peerlings, R.H.J., de Borst, R., Brekelmans, W.A.M., Geers, M., 1998. Gradient enhanced damage modelling of concrete fracture. International Journal for Numerical and Analytical Methods in Geomechanics 3, 323–342.

Peerlings, R.H.J., Geers, M.G.D., de Borst, R., Brekelmans, W.A.M., 2001. A critical comparison of nonlocal and gradient-enhanced softening continua. International Journal of Solids and Structures 38, 7723–7746.

Pegon, P., Anthoine, A., 1997. Numerical strategies for solving continuum damage problems with softening: application to the homogenization of masonry. Computers and Structures 64, 623–642.

Pijaudier-Cabot, G., Bažant, Z., 1987. Nonlocal damage theory. Journal of Engineering Mechanics 113, 1512–1533.

Pijaudier-Cabot, G., Dufour, F., 2010. Nonlocal damage model: boundary and evolving boundary effects. European Journal of Environmental and Civil Engineering 14 (6–7), 729–749.

Pijaudier-Cabot, G., Haidar, K., Dubé, J.-F., 2004. Non-local damage model with evolving internal length. International Journal for Numerical and Analytical Methods in Geomechanics 28 (7–8), 633–652.

Rizzi, E., Carol, I., Willam, K., 1995. Localization analysis of elastic degradation with application to scalar damage. Journal of Engineering Mechanics 121 (4), 541–554.

Rodríguez-Ferran, A., Huerta, A., 2000. Error estimation and adaptivity for nonlocal damage models. International Journal of Solids and Structures 37 (48–50), 7501–7528.

Simone, A., Askes, H., Sluys, L.J., 2004. Incorrect initiation and propagation of failure in non-local and gradient-enhanced media. International Journal of Solids and Structures 41, 351–363.

Verpeaux, P., Charras, T., Millard, A., 1988. Castem 2000 une approche moderne du calcul des structures. In: Fouet, J.M., LadevFze, P., Ohayon, R., (Eds.), Calcul des Structures et Intelligence Artificielle, Pluralis, pp. 261–271.

Voyiadjis, G., Abu Al-Rub, R., 2005. Gradient plasticity theory with a variable length scale parameter. International Journal of Solids and Structures 42 (14), 3998–4029.